

# Effects of grain size distribution on the interstellar dust mass growth

Hiroyuki Hirashita<sup>1\*</sup> and Tzu-Ming Kuo<sup>1,2</sup>

<sup>1</sup>*Institute of Astronomy and Astrophysics, Academia Sinica, P.O. Box 23-141, Taipei 10617, Taiwan*

<sup>2</sup>*Department of Physics, National Taiwan University, Taipei 10617, Taiwan*

2011 May 23

## ABSTRACT

Grain growth by the accretion of metals in interstellar clouds (called ‘grain growth’) could be one of the dominant processes that determine the dust content in galaxies. The importance of grain size distribution for the grain growth is demonstrated in this paper. First, we derive an analytical formula that gives the grain size distribution after the grain growth in individual clouds for any initial grain size distribution. The time-scale of the grain growth is very sensitive to grain size distribution, since the grain growth is mainly regulated by the surface to volume ratio of grains. Next, we implement the results of grain growth into dust enrichment models of entire galactic system along with the grain formation and destruction in the interstellar medium, finding that the grain growth in clouds governs the dust content in nearby galaxies *unless* the grain size is strongly biased to sizes larger than  $\sim 0.1 \mu\text{m}$  or the power index of the grain size distribution is shallower than  $\sim -2.5$ . The grain growth in clouds contributes to the rapid increase of dust-to-gas ratio at a certain metallicity level (called critical metallicity in Asano et al. 2011 and Inoue 2011), which we find to be sensitive to grain size distribution. Thus, the grain growth efficiently increase the dust mass not only in nearby galaxies but also in high-redshift quasars, whose metallicities are larger than the critical value. Our recipe for the grain growth is applicable for any grain size distribution and easily implemented into any framework of dust enrichment in galaxies.

**Key words:** dust, extinction — galaxies: dwarf — galaxies: evolution — galaxies: ISM — galaxies: spiral — ISM: clouds

## 1 INTRODUCTION

In the interstellar medium (ISM), dust grains are the most efficient absorber of stellar light. The spectral energy distributions and the radiative heating and cooling in galaxies are thus strongly regulated by the presence of dust (e.g. Yamasawa et al. 2011). This means that the understanding of dust enrichment in galaxies is crucial in the studies of galaxy evolution.

Dust enrichment in galaxies is governed by various processes depending on age, metallicity, etc. (Dwek 1998). In the earliest stage of galaxy evolution, dust is predominantly produced by supernovae (SNe) (e.g. Kozasa et al. 2009), while at later epochs asymptotic giant branch (AGB) stars also contribute (Valiante et al. 2009). The time-scale of dust destruction by SN shocks is a few  $\times 10^8$  yr (Jones, Tielens, & Hollenbach 1996; Serra Díaz-Cano & Jones 2008), while that of dust supply from stellar sources is longer than 1 Gyr in the Milky Way (McKee 1989). Therefore, dust grains should grow in the ISM by the accretion of metals onto grains (Draine 2009) to explain the existence of dust in the ISM. The growth occurs most efficiently in molecular clouds, where the typical number density of hydrogen molecules is  $\sim 10^3 \text{ cm}^{-3}$  (Hirashita 2000a). This process is called ‘grain

growth in clouds’ in this paper. Observational pieces of evidence for the grain growth in clouds come from larger depletion of metal elements in cold clouds than in warm medium (Savage & Sembach 1996).

A lot of chemical evolution models treat the evolution of dust content in galaxies. These models usually include dust production by stars, grain growth in clouds, and dust destruction by SNe (e.g. Dwek 1998; Inoue 2003; Zhukovska, Gail, & Tieloff 2008; Calura, Pipino, & Matteucci 2008; Asano et al. 2011). Most of the models which consider the grain growth in clouds indicate that this process dominates the dust budget at sub-solar or solar metallicities. The grain growth occurs through the accretion of metals, so that the increasing rate of grain mass by the accretion of metals is proportional not only to the metallicity but also to the grain surface-to-volume ratio, which is very sensitive to the grain size distribution.

Most models so far assume a certain grain size distribution or a typical grain size to estimate the surface-to-volume ratio. However, since the dominant processes governing the grain size distribution should vary with age and metallicity (O’Donnell & Mathis 1997; Hirashita et al. 2010; Yamasawa et al. 2011), it is expected that a variety of grain size distributions emerge in a complex way depending on age and metallicity. The first source of dust in the history of galaxy evolution is SNe, and the dust grains produced by

\* E-mail: hirashita@asiaa.sinica.edu.tw

SNe are possibly biased to large ( $\gtrsim 0.1 \mu\text{m}$ ) sizes because small grains tend to be destroyed in the shocked region within SNe before being injected into the interstellar space (Bianchi & Schneider 2007; Nozawa et al. 2007). Hirashita et al. (2010) show that small grains are produced by shattering driven by interstellar turbulence if the dust abundance is as high as that expected from the solar metallicity. Jones et al. (1996) show that shattering in interstellar SN shocks increases the abundance of small grains. Efficient production of small grains enhances the surface-to-volume ratio, activating the grain growth by the accretion of metals. Thus, we should consider various grain size distributions depending on galaxy age and metallicity, and the grain growth efficiency may vary with a variety of grain size distributions.

The first aim of this paper is to formulate the grain growth in clouds by explicitly considering the dependence on grain size distribution. Therefore, the former part of this paper is devoted to the formulation of the grain growth in clouds under an arbitrary grain size distribution. Then, by using this formulation, we point out the importance of grain size distribution for the grain growth by accretion. The final scope of this work is to examine if the grain size distribution has a significant influence on the dust enrichment in galaxies through the grain growth in clouds. Thus, in the latter part of this paper, we implement our formulation of the grain growth in clouds into a simple framework of dust enrichment in a galaxy, also taking into account the grain formation by stellar sources and the destruction by interstellar shocks driven by SN remnants. Thereby, we will show that our formulation of dust growth is successfully incorporated into dust enrichment models, and we will address the importance of grain size distribution for the grain mass budget in galaxies.

This paper is organized as follows. We explain the formulation in Section 2, and describe some basic results on the evolution of grain size distribution through the grain growth in individual clouds in Section 3. We implement the results for the grain growth in clouds into a simple evolution model of dust mass in an entire galactic system in Section 4, where the model also treats the dust formation by stellar sources and the dust destruction by SN shocks. We discuss the results in more general contexts in Section 5. Finally, Section 6 gives the conclusion.

## 2 FORMULATION

In this section, we formulate the evolution of grain size distribution by the accretion of metals (grain growth) in a single interstellar cloud. Our procedures in this paper are divided into the following two steps: (i) we construct a formulation of the grain growth in clouds, which is conveniently incorporated in any dust evolution models in galaxies; and (ii) we show that our formulation in this section can be used generally to treat the grain growth in galaxies. This section is aimed at item (i). In Section 4, we address item (ii) by incorporating our formulation for the grain growth into simple dust enrichment models which also include dust formation by stellar sources and dust destruction in SN shocks. Other mechanisms that modify the grain size distribution such as shattering and coagulation are treated in other papers (Jones et al. 1994, 1996; Yan et al. 2004; Hirashita & Yan 2009; Yamasawa et al. 2011). These processes are to be included in future work for the comprehensive understanding of the evolution of grain size distribution.

Throughout this paper, we call the elements composing grains ‘metals’. We only treat grains refractory enough to survive after the dispersal of the cloud, and do not consider volatile grains such

as water ice. More specifically, we consider silicate and graphite as main dust components. We also assume that the grains are spherical with a constant material density  $s$ , so that the grain mass  $m$  and the grain radius  $a$  are related as

$$m = \frac{4}{3}\pi a^3 s. \quad (1)$$

### 2.1 Evolution of grain size distribution

We define the grain size distribution such that  $n(a, t) da$  is the number density of grains whose radii are between  $a$  and  $a + da$  at time  $t$ . For simplicity, we assume that the gas density is constant and the evolution of grain size distribution occurs only through the accretion of metals on dust grains. In this situation, the number density of grains is conserved. Thus, the following continuity equation in terms of  $n(a, t)$  holds:

$$\frac{\partial n(a, t)}{\partial t} + \frac{\partial}{\partial a} [n(a, t) u] = 0, \quad (2)$$

where  $u \equiv da/dt$  is the growth rate of the grain radius and is given in the next subsection. Coagulation and shattering, which do not conserve the number density of grains, are not treated to focus on the grain growth by accretion here. Note that these processes do not change the grain mass, while the grain growth by accretion increases it. The evolution of grain size distribution by coagulation and shattering is treated in other papers (Jones et al. 1996; Hirashita & Yan 2009; Ormel et al. 2009). We also neglect possible grain destruction mechanisms in molecular clouds by cosmic rays or shocks.

### 2.2 Grain growth rate

The grain growth rate is basically determined by the collision rate between a grain and particles of the relevant metal species. We adopt silicate and graphite as dominant grain species (e.g. Draine & Lee 1984), and denote elements composing the grains as  $X$  (for example,  $X = \text{C}, \text{Si}$ , etc.). We neglect the effect of Coulomb interaction on the cross section (i.e. the cross section of a grain for accretion of metals is simply estimated by the geometric one) because the grains and the atoms are neutral in molecular clouds (Weingartner & Draine 1999; Yan et al. 2004). In fact, the ionization degree in dense clouds is  $10^{-6}$  (Yan et al. 2004), which means that almost all the metal atoms colliding with the dust grains are neutral. The rate at which atoms of element  $X$  strike the surface of a grain with radius  $a$  is denoted as  $\mathcal{R}$  and is estimated as (Evans 1994)

$$\mathcal{R} = 4\pi a^2 n_X \left( \frac{kT_{\text{gas}}}{2\pi m_X} \right)^{1/2}, \quad (3)$$

where  $n_X$  is the number density of element  $X$ ,  $k$  is the Boltzmann constant,  $T_{\text{gas}}$  is the gas temperature, and  $m_X$  is the atom mass of element  $X$ . In general, dust grains are not composed of a single species. We adopt a key element, whose mass fraction in the grain material is  $f_X$ , and represent the grain growth by the accretion of element  $X$ . The concept of key element is also adopted by Zhukovska et al. (2008).

By using  $f_X$ , the increase of the grain mass  $m$  is estimated as

$$\frac{dm}{dt} = f_X^{-1} m_X S \mathcal{R}, \quad (4)$$

where  $S$  is the sticking probability. This equation is converted into

the increasing rate of  $a$  by using equations (1) and (3) as

$$u = \frac{da}{dt} = \frac{n_X(t) m_X S}{f_X s} \left( \frac{kT_{\text{gas}}}{2\pi m_X} \right)^{1/2}. \quad (5)$$

In fact,  $n_X(t)$  is a function of time because the metal abundance in gas phase decreases as the dust grains grow. This effect is treated in the next subsection.

### 2.3 Depletion of gas-phase metals

The decreasing rate of the number density of element X in gas phase is equal to the grain growth rate per volume:

$$\frac{dn_X}{dt} = - \int_0^\infty \mathcal{R} S n(a, t) da. \quad (6)$$

Now we introduce the  $\ell$ -th moment of  $a$  as

$$\langle a^\ell \rangle(t) \equiv \frac{1}{n_d} \int_0^\infty a^\ell n(a, t) da, \quad (7)$$

where  $n_d$  is the number density of dust grains, which is independent of  $t$ :

$$n_d \equiv \int_0^\infty n(a, t) da. \quad (8)$$

The moments are functions of  $t$ , and their values at  $t = 0$  are denoted as  $\langle a^\ell \rangle_0 \equiv \langle a^\ell \rangle(0)$ . By using the second moment of  $a$  and equation (3) for  $\mathcal{R}$ , equation (6) can be expressed as

$$\frac{dn_X}{dt} = -4\pi n_X(t) S \left( \frac{kT_{\text{gas}}}{2\pi m_X} \right)^{1/2} n_d \langle a^2 \rangle(t). \quad (9)$$

Note that the third moment of  $a$  is related to the dust mass density  $\rho_d(t)$  as

$$\rho_d(t) = \frac{4}{3} \pi \langle a^3 \rangle(t) s n_d. \quad (10)$$

The initial dust mass density is  $\rho_d(0) = \frac{4}{3} \pi \langle a^3 \rangle_0 s n_d$ .

Here we quantify the initial number density of element X. The total number density of element X both in gas and dust phases is written as

$$n_{X,\text{tot}} \equiv \left( \frac{Z}{Z_\odot} \right) \left( \frac{X}{H} \right)_\odot n_H, \quad (11)$$

where  $Z$  is the metallicity, and  $(X/H)_\odot$  is the solar abundance relative to hydrogen in number, and  $n_H$  is the number density of hydrogen nuclei. We denote the initial fraction of element X in gas phase as  $\xi$ :

$$n_X(0) = \xi n_{X,\text{tot}}. \quad (12)$$

Since the initial number density of element X in dust phase is  $f_X \rho_d(0)/m_X$ ,

$$\frac{f_X \rho_d(0)}{m_X} = (1 - \xi) n_{X,\text{tot}}. \quad (13)$$

By using equation (10) at  $t = 0$ , equation (13) is written as

$$1 - \xi = \frac{\frac{4}{3} \pi \langle a^3 \rangle_0 f_X s n_d}{m_X n_{X,\text{tot}}}. \quad (14)$$

Thus, the normalization of the grain size distribution is determined by

$$n_d = \frac{m_X (1 - \xi)}{\frac{4}{3} \pi \langle a^3 \rangle_0 f_X s} \left( \frac{Z}{Z_\odot} \right) \left( \frac{X}{H} \right)_\odot n_H, \quad (15)$$

where we used equation (11) for  $n_{X,\text{tot}}$ .

### 2.4 Formal solution

The most important characteristics of the grain growth by accretion is that the increasing rate of  $a$  is independent of  $a$  (equation 5). Thus, equation (2) gives a formal solution as

$$n(a, t) = n(a - A(t), 0), \quad (16)$$

where

$$A(t) \equiv \frac{m_X S}{f_X s} \left( \frac{kT_{\text{gas}}}{2\pi m_X} \right)^{1/2} \int_0^t n_X(t) dt. \quad (17)$$

$A(t)$  is obtained if we give  $n_X(t)$  by using equation (9). We formally assume that  $n(a, 0) = 0$  for  $a < 0$  so that equation (16) can be used even for  $a - A(t) < 0$ .

We introduce the following indicator for the dust mass increase in the cloud (equation 10):

$$\begin{aligned} \frac{\rho_d(t)}{\rho_d(0)} &= \frac{\langle a^3 \rangle(t)}{\langle a^3 \rangle_0} \\ &= \frac{\langle a^3 \rangle_0 + \langle a^2 \rangle_0 A(t) + \langle a \rangle_0 A(t)^2 + A(t)^3}{\langle a^3 \rangle_0}, \end{aligned} \quad (18)$$

where we expand the third moment by using equation (16). Note that the dust mass in the cloud at  $t$  is  $\langle a^3 \rangle(t)/\langle a^3 \rangle_0$  times the initial dust mass. A similar equation is also obtained for the grain mantle growth as shown by Guillet, Pineau des Forêts, & Jones (2007).

### 2.5 Typical time-scale

For numerical calculations and interpretations of the results, introducing a typical time-scale is convenient. The typical time-scale of grain growth by accretion is defined by

$$\tau \equiv a_0 / \left[ \frac{m_X n_{X,\text{tot}} S}{f_X s} \left( \frac{kT_{\text{gas}}}{2\pi m_X} \right)^{1/2} \right], \quad (19)$$

where  $a_0$  is a typical grain radius given arbitrarily. By using  $\tau$ , equation (17) is reduced to

$$A(t) = \frac{a_0}{\tau} \frac{1}{n_{X,\text{tot}}} \int_0^t n_X(t) dt, \quad (20)$$

while equation (9) is written as

$$\frac{dn_X(t)}{dt} = - \frac{3n_X a_0}{\tau} (1 - \xi) \frac{\langle a^2 \rangle(t)}{\langle a^3 \rangle_0}, \quad (21)$$

where we have used equation (14). Note that

$$\langle a^2 \rangle(t) = \langle a^2 \rangle_0 + 2\langle a \rangle_0 A(t) + A(t)^2. \quad (22)$$

A set of equations (20)–(22) is solved to obtain the grain growth  $A(t)$ .

### 2.6 Selection of quantities

We consider silicate and graphite as representative grain components (Draine & Lee 1984). In order to avoid the complexity arising from compound species, we treat those two species separately as a first approximation. The quantities adopted in this paper are summarized in Table 1.

Jones & Nuth (2011) point out that the accretion of Si, Fe, and Mg in the presence of abundant  $\text{H}_2$ , CO and  $\text{H}_2\text{O}$  may lead to formation of a complex ice. Therefore, the real picture of the silicate growth in clouds may be chemically complicated. They also state

**Table 1.** Adopted quantities.

Species	X	$f_X$	$m_X$ [amu]	$(X/H)_\odot$	$s$ [g cm <sup>-3</sup> ]
Silicate	Si	0.166	28.1	$3.55 \times 10^{-5}$	3.3
Graphite	C	1	12	$3.63 \times 10^{-4}$	2.26

that any silicate materials produced in the ISM with reasonable scenarios do not show the spectral properties actually observed in the ISM. For carbonaceous dust, graphite and amorphous carbon have different chemical properties, leading to different growth properties in accretion. In this paper, because the knowledge about chemical properties is still poor, we simplify the picture by assuming that the grain growth is regulated by the sticking of the key species.

### 2.6.1 Silicate

We assume that the accretion of silicon regulates the growth of silicate grains. A larger abundance of oxygen is compensated by a larger number required to compose silicate. Zhukovska et al. (2008) also consider Mg as well as Si as a key species. The abundances of Mg and Si are almost the same if we assume the solar abundance pattern. Therefore, the following result does not change significantly even if we adopt O or Mg as a key element.

The solar abundance of Si is  $(\text{Si}/\text{H})_\odot = 4.07 \times 10^{-5}$  (Lodders 2003), and the mass of a Si atom is  $m_{\text{Si}} = 28.1$  amu (1 amu =  $1.66 \times 10^{-24}$  g). For the material properties of silicate, we assume  $s = 3.3$  g cm<sup>-3</sup> and  $f_{\text{Si}} = 0.166$  based on composition  $\text{Mg}_{1.1}\text{Fe}_{0.9}\text{SiO}_4$  (Draine & Lee 1984). By using equation (11), the typical time-scale  $\tau$  (equation 19) can be estimated as

$$\tau = 6.30 \times 10^7 a_{0.1} (Z/Z_\odot)^{-1} n_3^{-1} T_{50}^{-1/2} S_{0.3}^{-1} \text{ yr}, \quad (23)$$

where  $a_{0.1} \equiv a_0/0.1 \mu\text{m}$ ,  $n_3 \equiv n_{\text{H}}/10^3 \text{ cm}^{-3}$ ,  $T_{50} \equiv T_{\text{gas}}/50 \text{ K}$ , and  $S_{0.3} \equiv S/0.3$ . Unless otherwise stated, we adopt  $n_{\text{H}} = 10^3 \text{ cm}^{-3}$  and  $T = 50 \text{ K}$  for the typical values derived from observational properties of Galactic molecular clouds (Hirashita 2000a), and  $S = 0.3$  (Leitch-Devlin & Williams 1985; Grassi et al. 2011). Although  $S$  may be almost 1 in such a low temperature environments as molecular clouds (Zhukovska et al. 2008), the chemical factor (i.e. if the stucked atom finally becomes the part of the grain or not) is quite difficult to quantify as noted above (Jones & Nuth 2011). Thus, we adopt a conservative value of  $S$  in this paper. In fact,  $\tau$  depends on  $ZS$ , so a larger value of  $S$  is compensated by a smaller  $Z$ . In other words, the same dust growth rate is achieved with metallicity  $Z/(S/0.3)$  if we adopt a different value of  $S$ . Similar discussion also holds for the other quantities ( $T$  and  $n$ ).

### 2.6.2 Graphite (carbonaceous grains)

The solar abundance of C is  $(\text{C}/\text{H})_\odot = 2.88 \times 10^{-4}$  (Lodders 2003) and the mass of a C atom is  $m_{\text{C}} = 12$  amu. For graphite, we assume  $s = 2.26$  g cm<sup>-3</sup> (Draine & Lee 1984) and  $f_{\text{C}} = 1$  (i.e. graphite is solely composed of C). The typical time-scale is

$$\tau = 5.59 \times 10^7 a_{0.1} (Z/Z_\odot)^{-1} n_3^{-1} T_{50}^{-1/2} S_{0.3}^{-1} \text{ yr}. \quad (24)$$

If we adopt other carbon species such as amorphous carbon, the time-scale does not change as long as  $s$  is similar. If a light material like hydrogenated amorphous carbon (a-C:H) ( $s = 1.3\text{--}1.5$  g cm<sup>-3</sup> and  $f_{\text{C}} = 0.91\text{--}0.98$ ; Serra Díaz-Cano & Jones 2008) is adopted,  $\tau$  becomes 0.52–0.65 times the above value. The face value of  $\tau$

indicates that a-C:H grains grow more efficiently than graphite, although the difference in  $S$  between these two species is not clear. The destruction of a-C:H is, however, also more efficient than that of graphite (Serra Díaz-Cano & Jones 2008).

## 2.7 Initial grain size distribution

We examine a variety of initial grain size distributions. The various models surveyed are called Models A–H as listed in Table 2.

### 2.7.1 Single size ( $\delta$ function)

We first examine the case where the grain size distribution is strongly peaked at a certain typical radius. For example, dust grains condensed in SNe have a typical radius of  $\sim 0.1 \mu\text{m}$  if the shock efficiently destroys smaller grains (Bianchi & Schneider 2007; Nozawa et al. 2007). Here, the typical radius is assumed to be  $a_0$ , and  $\delta$  function is adopted for the grain size distribution for simplicity. Then we obtain

$$n(a, 0) = n_d \delta(a - a_0), \quad (25)$$

where  $n_d$  is given by equation (15). The moments are  $\langle a^\ell \rangle_0 = a_0^\ell$ .

### 2.7.2 Power law

If the grain size distribution is described by a power law, the typical grain size is not obvious. Thus, we arbitrarily adopt  $a_0 = 0.1 \mu\text{m}$  for power-law grain size distributions. The upper and lower bounds for the grain radii are denoted as  $a_{\min}$  and  $a_{\max}$ , respectively:

$$n(a, 0) = \begin{cases} \frac{(1-r)n_d}{(a_{\max}^{1-r} - a_{\min}^{1-r})} a^{-r} & (r \neq 1); \\ \frac{n_d}{\ln(a_{\max}/a_{\min})} a^{-r} & (r = 1); \end{cases} \quad (26)$$

for  $a_{\min} \leq a \leq a_{\max}$ . If  $a < a_{\min}$  or  $a > a_{\max}$ ,  $n(a, 0) = 0$ . The normalization  $n_d$  is given by equation (15).

The moments are given by

$$\langle a^\ell \rangle_0 = \begin{cases} \frac{1-r}{\ell+1-r} \frac{a_{\max}^{\ell+1-r} - a_{\min}^{\ell+1-r}}{a_{\max}^{1-r} - a_{\min}^{1-r}} & (r \neq 1, \ell+1); \\ \frac{1}{\ell} \frac{a_{\max}^\ell - a_{\min}^\ell}{\ln(a_{\max}/a_{\min})} & (r = 1); \\ \frac{-\ell}{a_{\max}^{-\ell} - a_{\min}^{-\ell}} \ln(a_{\max}/a_{\min}) & (r = \ell+1). \end{cases} \quad (27)$$

## 3 GRAIN GROWTH IN INDIVIDUAL CLOUDS

First, we examine single size cases (Models A and B), where the grain size distribution is described by  $\delta$  function. For the initial fraction of element X in gas phase, we adopt  $\xi = 0.5$  and 0.9 as representative cases where a moderate fraction and only a small fraction of metals are in dust phase, respectively. In Fig. 1, we show the evolution of  $n_X(t)/n_{X,\text{tot}}$  and  $\langle a^3 \rangle(t)/\langle a^3 \rangle_0$  for Models A and B. Note that  $\langle a^3 \rangle(t)/\langle a^3 \rangle_0$  is proportional to the dust mass or the dust mass density (equation 18) and that  $n_X(t=0)/n_{X,\text{tot}} = \xi$  (the fraction of metals in gas phase at  $t = 0$ ). As the model imposes, the dust mass increases with the depletion of gas-phase metals onto the grains. For larger  $\xi$ , the grains continue to grow to larger radii and for a longer time, since the available metals in gas phase is more abundant and the abundance of dust relative to the

**Table 2.** Models.

Model	$n^a$	$a_0$ [ $\mu\text{m}$ ]	$\xi$	$r$	$a_{\min}$ [ $\mu\text{m}$ ]	$a_{\max}$ [ $\mu\text{m}$ ]	$\langle a \rangle_0^c$ [ $\mu\text{m}$ ]	$\sqrt{\langle a^2 \rangle_0^c}$ [ $\mu\text{m}$ ]	$\sqrt[3]{\langle a^3 \rangle_0^c}$ [ $\mu\text{m}$ ]	$\langle a^3 \rangle_0 / \langle a^2 \rangle_0^c$ [ $\mu\text{m}$ ]
A	$\delta$	— <sup>b</sup>	0.5	—	—	—	—	—	—	—
B	$\delta$	— <sup>b</sup>	0.9	—	—	—	—	—	—	—
C	p	0.1	0.5	3.5	0.001	0.25	0.00167	0.00216	0.00402	0.0159
D	p	0.1	0.5	2.5	0.001	0.25	0.00281	0.00667	0.0158	0.0887
E	p	0.1	0.5	4.5	0.001	0.25	0.00140	0.00153	0.00187	0.00279
F	p	0.1	0.9	3.5	0.001	0.25	0.00167	0.00216	0.00420	0.0159
G	p	0.1	0.5	3.5	0.0003	0.25	0.000499	0.000659	0.00156	0.00874
H	p	0.1	0.9	3.5	0.003	0.25	0.00499	0.00633	0.0103	0.0273

<sup>a</sup> Initial grain size distribution: “p” for the power law and “ $\delta$ ” for the  $\delta$  function.

<sup>b</sup> The time-scale is scalable for any  $a_0$  by using equations (23) and (24).

<sup>c</sup> The moments of  $a$  are not free parameters but are calculated once the other parameters are fixed.

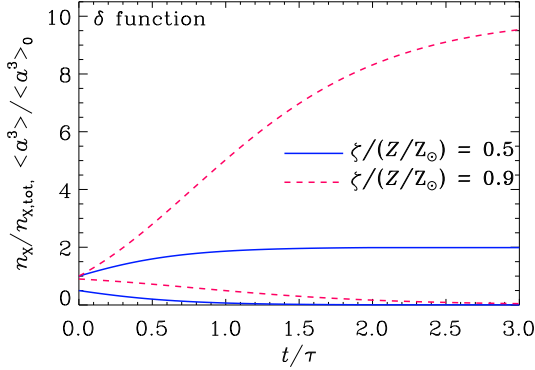


**Figure 1.** Evolutions of the normalized grain volume (or mass) relative to the initial value,  $\langle a^3 \rangle / \langle a^3 \rangle_0$ , and the number density of element X in gas phase normalized to the total (gas phase + dust phase) number density,  $n_X / n_{X,\text{tot}}$ , along with the normalized time  $t/\tau$ . The  $\delta$  function grain size distribution is adopted. Solid and dashed lines show the results of Models A and B, respectively (i.e.  $\xi = 0.5$  and  $0.9$ , respectively) with the upper and lower lines show the evolution of  $\langle a^3 \rangle / \langle a^3 \rangle_0$  and  $n_X / n_{X,\text{tot}}$ , respectively.

gas phase metals is smaller. At  $t \gg \tau$ ,  $\langle a^3 \rangle(t) / \langle a^3 \rangle_0$  approaches  $1/(1 - \xi)$ , which means that the grain mass becomes  $1/(1 - \xi)$  times the initial mass after all the gas phase X is depleted onto the dust grains.

Next, we examine the power-law grain size distributions (Models C–H in Table 2). Mathis, Rumpl, & Nordsieck (1977, hereafter MRN) show that the extinction curve in the Milky Way can be fitted with a power-law grain size distribution. We fix the range of the grain size by adopting  $a_{\min} = 0.001 \mu\text{m}$ , and  $a_{\max} = 0.25 \mu\text{m}$  (MRN). We arbitrarily fix the value of  $a_0$  as  $a_0 = 0.1 \mu\text{m}$  (Section 2.7.2). Since the lower bound of the grain size is poorly determined from the extinction curve (Weingartner & Draine 2001), we also examine the case where the smallest radius is  $0.0003 \mu\text{m}$  ( $3 \text{ \AA}$ ). We change the power-law index  $r$  from 2.5 to 4.5 to examine the cases where large and small grains are relatively dominated, respectively (note that  $r = 3.5$  corresponds to MRN). We also vary  $\xi$ .

In Fig. 2, we show the results for Models C–E. As shown in equation (21), the consumption rate of metals in gas phase is pro-

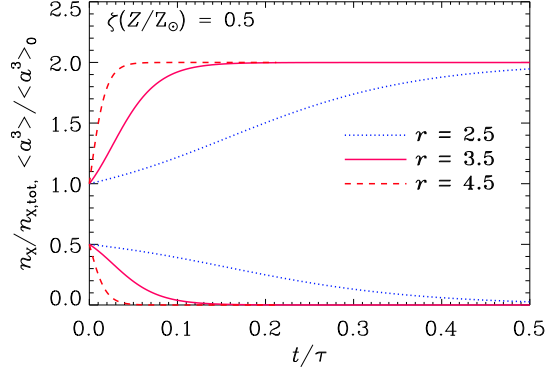


**Figure 2.** Same as Fig. 1 but for the power-law initial grain size distributions (Models C–E). Solid, dotted, and dashed lines show the results of Models C, D, and E ( $r = 3.5$ ,  $2.5$ , and  $4.5$ ), respectively with the upper and lower lines show the evolution of  $\langle a^3 \rangle / \langle a^3 \rangle_0$  and  $n_X / n_{X,\text{tot}}$ , respectively.

portional to the surface-to-volume ratio of dust grains. If  $r$  is large, the surface-to-volume ratio is large, so that the metals in gas phase is rapidly consumed onto dust grains.

Fig. 3 illustrates the evolution of grain size distribution. To show the mass distribution per logarithmic size, we multiply  $a^4$  to  $n$ . Also in order to make the quantity dimensionless, we multiply  $a_0/n_d$ . We indeed observe that the small grains grow to larger grains. Since the increasing rate of grain radius is independent of  $a$ , the impact of grain growth is significant for small grains as already shown by Guillet et al. (2007) for the mantle growth. Moreover, gas-phase metals accrete selectively onto small grains (especially for larger  $r$ ) because the grain surface is dominated by small grains; this is consistent with the results of Weingartner & Draine (1999).

To show the dependence on  $\xi$ , we compare Models C and F. The results are shown in Fig. 4. Different values of  $\xi$  lead to different final-to-initial dust mass ratios  $\langle a^3 \rangle / \langle a^3 \rangle_0 \rightarrow 1/(1 - \xi)$ , which are interpreted in the same way as in the  $\delta$  function cases (Fig. 1).

Finally, in Fig. 5, we compare Models C, G, and H to examine the dependence on  $a_{\min}$ . As expected, the results are sensitive to  $a_{\min}$  since the surface-to-volume ratio of grains differs largely (Table 2) (see also Weingartner & Draine 1999). Therefore, it is important to specify the physics governing the smallest grain size

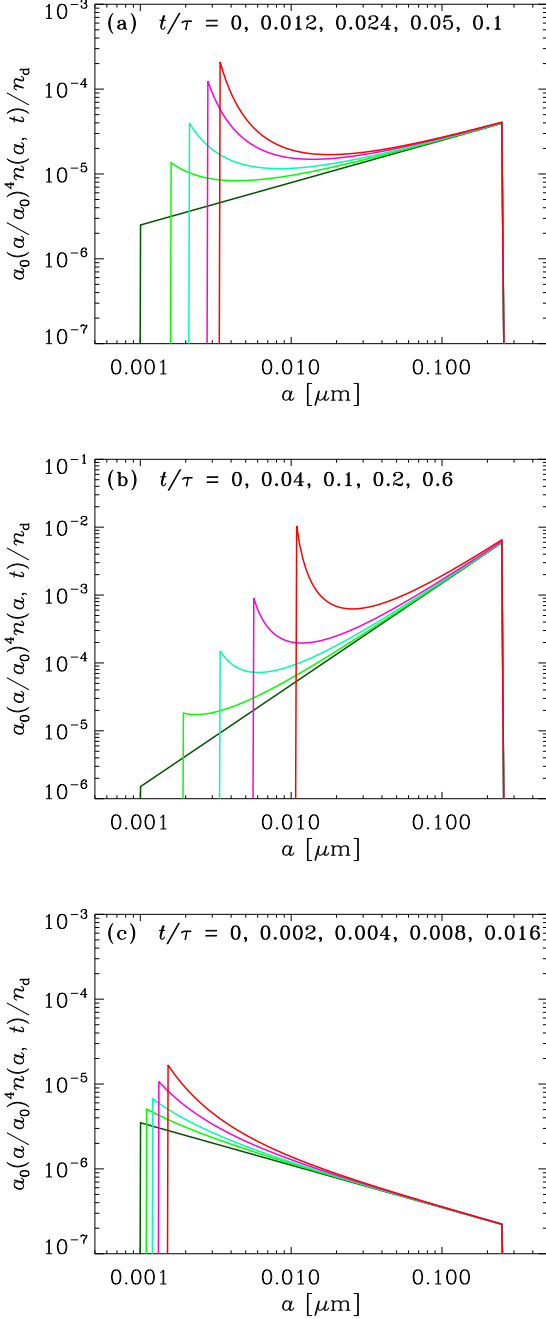


**Figure 3.** Evolution of grain size distribution for Models C, D, and E (Panels a, b, and c, respectively). The normalized times are shown in each panel. The size distribution is shown by  $a_0(a/a_0)^4 n(a, t)/n_d$  to indicate the normalized grain mass distribution per logarithmic size.

in interstellar clouds. Coagulation possibly depletes grains smaller than several Å (Hirashita & Yan 2009; Guillet et al. 2011).

#### 4 IMPLEMENTATION INTO GALAXY EVOLUTION MODELS

In this section, we relate the results above for the grain growth in individual clouds to the dust mass evolution in an entire galactic

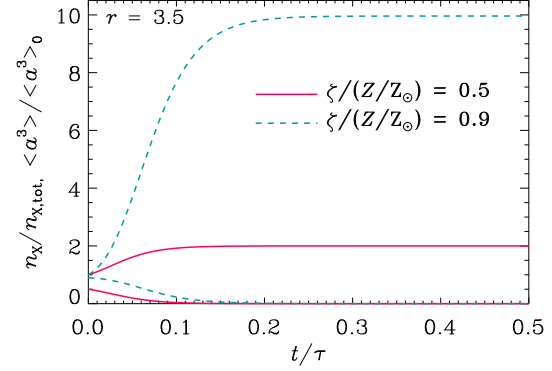


**Figure 4.** Same as Fig. 2 but for Models C and F ( $\xi = 0.5$  and  $0.9$ , respectively, with  $r = 3.5$ ).

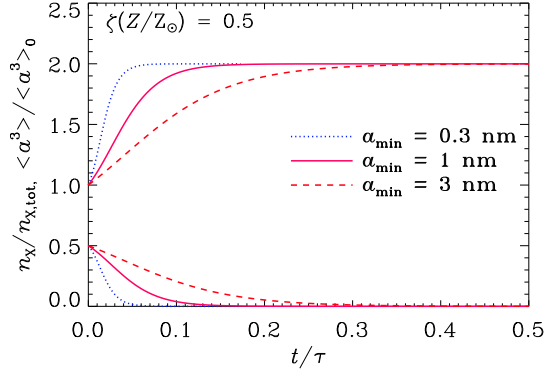


**Figure 5.** Same as Fig. 2 but for Models C, G, and H, where the minimum grain radius is varied as  $a_{\min} = 0.3, 1,$  and  $3$  nm, respectively, with  $r = 3.5$ .

system. We adopt a chemical evolution model that calculates the metal and dust enrichment. To concentrate on the importance of grain size distribution, we simplify the galaxy evolution models, although our recipe for the grain growth is simple enough to be easily implemented to more complicated galaxy evolution models. The entire galactic system is treated as one zone. The treatment of one zone is good if the dust, metals, and gas are mixed instantaneously or if we focus on a certain well mixed region in the galaxy. For example, in spiral galaxies which generally have a radial metallicity gradient, our models can be applicable to a certain radius range where the metallicity can be regarded as uniform.

Since we are interested in the effects on dust enrichment, we compare our results with the dust abundance in galaxies. Given that the dust enrichment is closely related with the metal enrichment, it is convenient to derive the relation between dust-to-gas ratio and metallicity (e.g. Lisenfeld & Ferrara 1998). The dust mass is usually estimated by the far-infrared emission to trace the emission from large grains, which occupy a significant fraction of the dust mass. The dust mass estimated from the far-infrared emission can miss very small grains and very cold dust. The contribution from very small grains to the dust mass is not significant (Désert, Boulanger, & Puget 1990; Galliano et al. 2005;

Compiègne et al. 2011). Very cold dust traced in longer wavelengths than submillimetre may have a significant contribution to the total dust mass especially in metal-poor galaxies (Galliano et al. 2003, 2005; Galametz et al. 2011), but its abundance is significantly affected by the assumed emissivity index of large grains. If we miss the contribution from very cold dust, the observational dust-to-gas ratio is underestimated in this paper, which enhances the importance of the dust growth in clouds to explain the additional contribution from very cold dust.

Although there is a large variety in the grain size distribution derived from the dust emission spectrum (Galliano et al. 2005), the regulation mechanism of grain size distribution in the ISM is not fully understood. Therefore, in this paper, we examine various grain size distributions (i.e.  $\delta$  function with various typical sizes and power law with various power indices). Sputtering and shattering in SN shocks (Jones et al. 1996) and shattering in interstellar turbulence (Yan, Lazarian, & Draine 2004; Hirashita et al. 2010) may play a significant role in determining the shape of grain size distribution. Inclusion of these processes into the evolution of grain size distribution is left for future work to concentrate on the grain growth in clouds in this paper. A simultaneous treatment of dust formation and destruction can be seen in Yamasawa et al. (2011).

Photo-processes are neglected in this paper. Dust may contain ice mantle when it is injected into the ISM from clouds. When the dust is exposed to stellar radiation, the evaporation of the ice mantle may lead to grain disaggregation. If small refractory grains are ejected in the disaggregation, the total amount of refractory dust (silicate and graphite in this paper) does not change, so that our conclusion below is not affected. If the dust is destroyed and the refractory elements are returned into the gas phase in the photo-processing, the dust abundance may be affected by this process. The destruction of dust by photo-processing, if any, can be effectively included into the dust destruction efficiency ( $\beta_{\text{SN}}$  defined later), but we will see later that only the destruction by SNe is enough to explain the dust-to-metal ratio (Section 5.2).

#### 4.1 Grain growth time-scale

We define the increased fraction of dust mass in a cloud,  $\beta$ , which is evaluated as

$$\begin{aligned} \beta &= \frac{\langle a^3 \rangle(\tau_{\text{cl}})}{\langle a^3 \rangle_0} - 1 \\ &= \frac{A(\tau_{\text{cl}})[3\langle a^2 \rangle_0 + 3\langle a \rangle_0 A(\tau_{\text{cl}}) + A(\tau_{\text{cl}})^2]}{\langle a^3 \rangle_0}, \end{aligned} \quad (28)$$

where  $\tau_{\text{cl}}$  is the lifetime of clouds hosting the grain growth and equation (18) is used from the second to the third step. The dust mass in the cloud becomes  $(\beta + 1)$  times the initial value after the cloud lifetime, when the dust grown in the cloud returns in the diffuse ISM (see equation 18).

Now we consider how to implement our results into dust enrichment models for an entire galactic system. By using  $\beta$ , the increasing rate of dust mass by accretion in clouds should be written as

$$\left[ \frac{dM_{\text{dust}}}{dt} \right]_{\text{acc}} = \frac{\beta X_{\text{cl}} M_{\text{dust}}}{\tau_{\text{cl}}}, \quad (29)$$

where  $M_{\text{dust}}$  is the total dust mass in the galaxy, and  $X_{\text{cl}}$  is the mass fraction of clouds hosting the grain growth to the total gas mass. In equation (29), we have assumed that the time-scale of dust enrichment is much longer than the cloud lifetime so that the mass increasing rate in each cloud is estimated by  $\beta/\tau_{\text{cl}}$  times the dust

mass in the cloud. On the other hand, Hirashita (2000a) express the increasing rate of the dust mass in a galaxy through the grain growth in clouds by

$$\left[ \frac{dM_{\text{dust}}}{dt} \right]_{\text{acc}} = \frac{X_{\text{cl}} M_{\text{dust}} \xi}{\tau_{\text{grow}}}, \quad (30)$$

where  $\tau_{\text{grow}}$  is the growth time-scale of the dust in a cloud, and  $\xi$  is the fraction of metals in gas phase (Section 2.2). A similar expression for the increasing rate of the dust mass is widely adopted in dust enrichment models (e.g. Dwek 1998; Inoue 2003; Calura et al. 2008).

Comparing equations (29) and (30), we obtain

$$\frac{\tau_{\text{grow}}}{\tau_{\text{cl}}} = \frac{\xi}{\beta} = \frac{\xi \langle a^3 \rangle_0}{A(\tau_{\text{cl}})[3\langle a^2 \rangle_0 + 3\langle a \rangle_0 A(\tau_{\text{cl}}) + A(\tau_{\text{cl}})^2]}, \quad (31)$$

where equation (28) is used for  $\beta$ . Thus, we obtain  $\tau_{\text{grow}}/\tau_{\text{cl}}$  as a function of  $\tau_{\text{cl}}$ ; that is, if we give the lifetime of molecular cloud, we can evaluate  $\tau_{\text{grow}}$ . Equation (20) indicates that  $A(\tau_{\text{cl}})$  depends on  $\tau$ . Since  $\tau$  depends on the metallicity (equations 23 and 24),  $\tau_{\text{grow}}/\tau_{\text{cl}}$  evolves as the system is enriched with metals. Here we adopt equation (23) for  $\tau$ . To simplify the discussion, we focus on the metallicity and the grain size distribution with the other quantities fixed; that is,  $\tau = 63.0 a_{0.1} (Z/Z_{\odot})^{-1}$  Myr. As a result, if we specify  $\tau_{\text{cl}}$  and give a grain size distribution, we obtain  $\tau_{\text{grow}}/\tau_{\text{cl}}$  as a function of  $Z/\tau_{\text{cl}}$ . Thus, we can regard  $\tau_{\text{grow}}/\tau_{\text{cl}}$  as a function of metallicity if we fix  $\tau_{\text{cl}}$ . The results are shown in Fig. 6.

Fig. 6 shows that  $\tau_{\text{grow}}/\tau_{\text{cl}}$  depends on the grain size distribution as expected from the results in the previous section. In particular, if  $a_0$  is smaller for the  $\delta$  function cases or  $r$  is larger in the power-law cases, the grains grow on a shorter time-scale so  $\tau_{\text{grow}}$  becomes smaller. We also observe the dependence on  $\xi$ : if  $\xi$  is larger, the grains grow to a larger extent because the abundance of available metals relative to dust is larger. Thus,  $\tau_{\text{grow}}/\tau_{\text{cl}}$  becomes smaller for larger  $\xi$  in the region of high  $Z$  or large  $\tau_{\text{cl}}$ .

Fig. 6 also shows that the behaviour at small metallicities is described by  $\tau_{\text{grow}} \propto Z^{-1}$ . This is explained as follows. If the metallicity is low enough,  $\tau_{\text{cl}} \ll \tau$ . Thus, the decrease of gas-phase metals is negligible, and equation (20) can be written as follows if we recall that  $n_{\text{X}}(0)/n_{\text{X,tot}} = \xi$ :

$$A(\tau_{\text{cl}}) \simeq \xi a_0 \tau_{\text{cl}}/\tau \quad \text{for } \tau_{\text{cl}} \ll \tau. \quad (32)$$

By taking up to the first order for  $\tau_{\text{cl}}/\tau$ , equation (31) is approximated as

$$\tau_{\text{grow}} \simeq \frac{\langle a^3 \rangle_0}{3\langle a^2 \rangle_0 a_0} \tau \propto Z^{-1} \quad \text{for } \tau_{\text{cl}} \ll \tau. \quad (33)$$

This indicates two important properties. One is that the grain growth time-scale (which is proportional to  $Z^{-1}$ ) is roughly determined by the typical growth time-scale  $\tau$  and the surface-to-volume ratio of dust grains. The other is that the cloud lifetime does not enter since the grain growth in each cloud during the cloud lifetime is slight enough.

As  $Z$  becomes large,  $\tau_{\text{grow}}/\tau_{\text{cl}}$  approaches a constant value independent of metallicity. Indeed, the grain growth saturates if the metals in gas phase are used out. Thus,  $\langle a^3 \rangle(\tau_{\text{cl}})/\langle a^3 \rangle_0 \rightarrow 1/(1 - \xi)$  as  $Z$  becomes large. In reality, the grain abundance in clouds would approach the value expected from the equilibrium between the grain growth and the destruction by cosmic ray, shocks, ultraviolet light in clouds, etc. We expect that the destruction within the clouds does not affect the dust abundance in the entire galaxy since the dominant destruction occurs in the diffuse ISM by SN shocks (McKee 1989). Thus, in the clouds, we only consider the

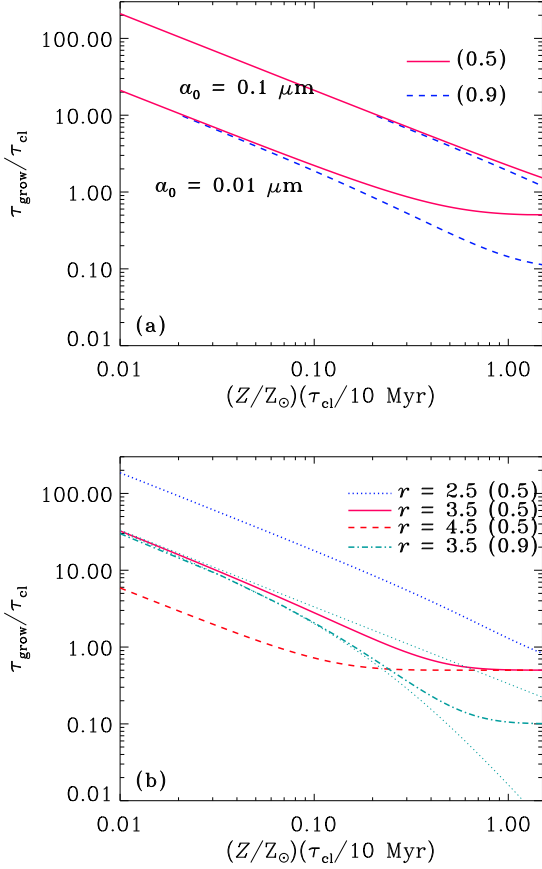


**Figure 6.** Ratio of the grain growth time-scale to the lifetime of clouds hosting the grain growth by accretion ( $\tau_{\text{grow}}/\tau_{\text{cl}}$ ) as a function of  $Z/Z_{\odot}$ . (a) The cases of single grain sizes ( $\delta$  function size distributions) are shown. The solid and dashed lines show the cases for  $\xi = 0.5$  and  $0.9$ , respectively. The upper and lower lines show the cases for  $a_0 = 0.1$  and  $0.01 \mu\text{m}$ , respectively. (b) The results for power-law grain size distributions are presented. The thick dotted, solid, and dashed lines are for  $r = 2.5, 3.5$ , and  $4.5$  with  $\xi = 0.5$ , while the dot-dashed line shows the case for  $r = 3.5$  with  $\xi = 0.9$ . The thin dotted lines show the relation predicted from equation (33) (upper line) and equation (31) with equation (32) (lower line) (the dot-dashed line is relevant for comparison).

grain growth and neglect dust destruction. In the dust enrichment model for the entire galaxy in Section 4.4, we include the dust destruction by SN shocks in diffuse medium. By using equation (31), we obtain

$$\tau_{\text{grow}} \simeq (1 - \xi)\tau_{\text{cl}} \quad (\text{for } \tau_{\text{cl}} \gg \tau), \quad (34)$$

where we note that  $\beta \simeq \xi/(1 - \xi)$  for  $\tau_{\text{cl}} \gg \tau$ . This result indicates that the grain growth is regulated by the cloud lifetime since the dust grains use up all the gas-phase metals within  $\tau_{\text{cl}}$ . The factor  $(1 - \xi)$  indicates that the dust mass increases with a larger fraction if a larger part of metals are in gas phase.

In Fig. 6b, we overlay the relation predicted by equation (33) for  $r = 3.5$  (the upper thin dotted line, which should be compared with the dot-dashed line for the exact solution). Although it gives a good approximation for low metallicities, the discrepancy becomes significant at  $(Z/Z_{\odot})(\tau_{\text{cl}}/10 \text{ Myr}) \gtrsim 0.1$ . This is because the increase of dust surface area by accretion further accelerates the accretion of gas phase metals. Such an effect of acceleration of

grain growth is not taken into account in deriving equation (33), but is included in the second and the third order terms of  $A$  in equation (31), where  $A$  can be approximated by equation (32) if the saturation of grain growth by the depletion of gas-phase metals is neglected. Thus, we expect that the approximation of  $\tau_{\text{grow}}$  becomes better than equation (33) if we combine equations (31) and (32). The result predicted by this combination is also shown in Fig. 6b (thin dotted line). It fits the exact solution better than equation (33), but it underestimates  $\tau_{\text{grow}}$  for large metallicities. This underestimate comes from the fact that we neglected the depletion of metals by the grain growth. This depletion effect occurs if the cloud lifetime is comparable or larger than the typical grain growth time-scale. Thus, we propose the following approximate formula to include the depletion effect:

$$\frac{\tau_{\text{grow}}}{\tau_{\text{cl}}} \simeq \frac{\xi \langle a^3 \rangle_0}{3y \langle a^2 \rangle_0 + 3y^2 \langle a \rangle_0 + y^3} + (1 - \xi), \quad (35)$$

where  $y \equiv a_0 \xi \tau_{\text{cl}}/\tau$  (Equation 32). In Fig. 7, we show this approximate formula in comparison with the exact results. We observe that the approximation is fairly good. By using equation (31),  $\beta = \xi(\tau_{\text{grow}}/\tau_{\text{cl}})^{-1}$ . Thus, we adopt the following approximation derived from equation (35):

$$\beta \simeq \left[ \frac{\langle a^3 \rangle_0}{3y \langle a^2 \rangle_0 + 3y^2 \langle a \rangle_0 + y^3} + \frac{1 - \xi}{\xi} \right]^{-1} \quad (36)$$

with  $y \equiv a_0 \xi \tau_{\text{cl}}/\tau$ . This approximate formula has a merit that we do not need to solve the differential equation for the depletion of gas-phase metals (equation 9). Therefore, we hereafter use equations (35) and (36) to estimate  $\tau_{\text{grow}}$  and  $\beta$ , respectively.

## 4.2 Relation to the star formation

Galaxies are enriched by metals and dust as a result of star formation activities. Thus, it is usually convenient to model the quantities in terms of the star formation. In fact, dust growth by accretion should be strongly related to star formation, since both occur predominantly in dense clouds in galaxies (Dwek 1998). Here we make use of  $\beta$  and connect the star formation rate with the grain growth rate by accretion.

If the fraction  $\epsilon$  of the cloud mass is converted into stars after the cloud lifetime  $\tau_{\text{cl}}$ , the star formation rate,  $\psi$ , is written as

$$\psi = \frac{\epsilon X_{\text{cl}} M_{\text{gas}}}{\tau_{\text{cl}}}, \quad (37)$$

where  $M_{\text{gas}}$  is the total gas mass in the galaxy. Then, equation (29) can be written by using the star formation rate as

$$\left[ \frac{dM_{\text{dust}}}{dt} \right]_{\text{acc}} = \frac{\beta \mathcal{D} \psi}{\epsilon}, \quad (38)$$

where  $\mathcal{D} \equiv M_{\text{dust}}/M_{\text{gas}}$  is the dust-to-gas ratio.

## 4.3 Recipe for implementation of grain growth

Here we summarize the recipe to include the grain growth by accretion into dust enrichment models. There are two methods as described in sections 4.1 and 4.2, called Method I and Method II, respectively.

**Method I** Assume  $X_{\text{cl}}$  (the mass fraction of clouds hosting grain growth) and  $\tau_{\text{cl}}$  (the lifetime of these clouds). Calculate also  $\langle a^\ell \rangle$  for  $\ell = 1, 2$ , and  $3$  for a given grain size distribution (or use the values in Table 2). Then, under any metallicity,  $\tau$  (the typical



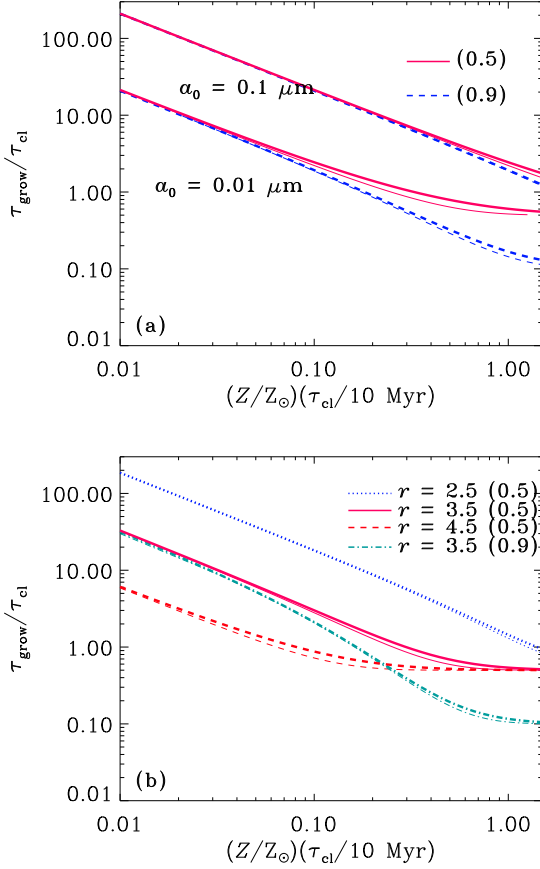


**Figure 7.** Same as Fig. 6 but we show the approximate results with equation (35). The thick lines show the approximate relations and, while the thin lines are calculated by the exact formulation used to produce the results in Fig. 6.

grain growth time-scale) is calculated by equation (23) for silicate, by equation (24) for graphite or by equation (19) in general, and  $y = a_0 \xi \tau_{cl} / \tau$  is also obtained. Note that  $\xi$  (the fraction of metals in gas phase) should be calculated within the framework of dust enrichment (Section 4.4). Finally use equation (31) (more conveniently equation 35 for an approximate formula) to obtain  $\tau_{grow}$ , which should be used in equation (30) to obtain  $[dM_{dust}/dt]_{acc}$ .

**Method II** Assume  $\tau_{cl}$  (the lifetime of clouds) and  $\epsilon$  (the star formation efficiency in these clouds). Calculate also  $\langle a^\ell \rangle$  for  $\ell = 1, 2$ , and 3 for a given grain size distribution (or use the values in Table 2). Then, under any metallicity,  $\tau$  is calculated by equation (23) for silicate or equation (24) for graphite, and  $y = a_0 \xi \tau_{cl} / \tau$  is also obtained. Note that  $\xi$  should be calculated by a chemical enrichment model. Finally use equation (28) (or more conveniently equation 36 for an approximate formula) to obtain  $\beta$ , which should be used in equation (38).

#### 4.4 Dust enrichment model

We demonstrate that our results so far are really implemented into galaxy evolution models with dust enrichment. The aim here is not to construct an elaborate chemical evolution model but to focus on the effect of grain growth. We adopt a one-zone closed-box model of dust/metal enrichment by Hirashita (2000b) (see also Dwek 1998; Lisenfeld & Ferrara 1998). The model treats the evolu-

tions of total gas, metals, and dust masses ( $M_{gas}$ ,  $M_Z$ , and  $M_{dust}$ , respectively) in the galaxy. In this model, the metals include not only gas phase elements but also dust. The equations are written as

$$\frac{dM_{gas}}{dt} = -\psi + E, \quad (39)$$

$$\frac{dM_Z}{dt} = -Z\psi + E_Z \quad (40)$$

$$\frac{dM_{dust}}{dt} = -\mathcal{D}\psi + f_{in}E_Z - \frac{M_{dust}}{\tau_{SN}} + \left[ \frac{dM_{dust}}{dt} \right]_{acc}, \quad (41)$$

where  $E$  and  $E_Z$  are the rate of the total injection of mass (gas + dust) and metal mass from stars, respectively,  $f_{in}$  is the dust condensation efficiency of the metals in the stellar ejecta, and  $\tau_{SN}$  is the time-scale of dust destruction by SN shocks. For simplicity, we do not treat individual element  $X$  but treat the entire metals; however, if we are interested in a specific dust-composing element  $X$ , we can replace the relevant quantities with ones specific for element  $X$ . The simple treatments above are sufficient to demonstrate that our scheme of grain growth in clouds for any grain size distribution is really applicable to the galaxy evolution models. We refer to other papers (e.g. Dwek 1998; Zhukovska et al. 2008; Gall et al. 2011a) for more detailed dust enrichment models.

Since we are not interested in the detailed history of dust production in stellar ejecta, we adopt the instantaneous recycling approximation; that is, a star with  $m > m_t$  ( $m$  is the zero-age stellar mass, and  $m_t$  is the turn-off mass at age  $t$ ) dies instantaneously after its birth, leaving a remnant of mass  $w_m$ . Once the initial mass function (IMF) is fixed, the returned fraction of the mass from formed stars,  $\mathcal{R}$ , and the mass fraction of metals that is newly produced and ejected by stars,  $\mathcal{Y}_Z$ , are evaluated. Using these quantities, we write

$$E = \mathcal{R}\psi, \quad (42)$$

$$E_Z = (\mathcal{R}Z + \mathcal{Y}_Z)\psi. \quad (43)$$

We adopt  $\mathcal{R} = 0.18$  and  $\mathcal{Y}_X = 0.013$  (Appendix). For  $f_{in}$ , we examine two cases:  $f_{in} = 0.1$  and  $0.01$ , which correspond to the fiducial and the lower efficiency cases in Inoue (2011), respectively.

For the time-scale of dust destruction by SNe, we adopt an expression  $\tau_{SN} = M_{gas} / (\epsilon_s M_s \gamma)$ , where  $\epsilon_s$  and  $M_s$  are the dust destruction efficiency and the gas mass swept by a single high-velocity SN blast, respectively, and  $\gamma$  is the SN rate (McKee 1989). Since we are interested in objects whose time-scale of star formation is much longer than  $10^7$  yr, it is assumed that the SN rate is proportional to the star formation rate (equation A6). We adopt  $\epsilon_s M_s = 1300 M_\odot$  (McKee 1989). Then we obtain

$$\tau_{SN} = \frac{M_{gas}}{\beta_{SN}\psi}, \quad (44)$$

where  $\beta_{SN} \equiv \epsilon_s M_s \gamma / \psi \simeq 9.65$ . As pointed out by Jones & Nuth (2011),  $\epsilon$  is uncertain by a factor of  $\sim 2$  and is dependent on the assumed grain composition (see also Serra Díaz-Cano & Jones 2008).

Equations (39)–(41) are converted to the time evolution of the metallicity  $Z = M_Z / M_{gas}$  and the dust-to-gas ratio  $\mathcal{D} = M_{dust} / M_{gas}$  as

$$\frac{M_{gas}}{\psi} \frac{dZ}{dt} = \mathcal{Y}_Z, \quad (45)$$

$$\frac{M_{gas}}{\psi} \frac{d\mathcal{D}}{dt} = f_{in}(\mathcal{R}Z + \mathcal{Y}_Z) - (\beta_{SN} + \mathcal{R})\mathcal{D} + \frac{1}{\psi} \left[ \frac{dM_{dust}}{dt} \right]_{acc}, \quad (46)$$

where we should evaluate  $[dM_{\text{dust}}/dt]_{\text{acc}}$  according to Method I or II in Section 4.3. It is convenient to combine the above two equations to obtain the relation between  $\mathcal{D}$  and  $Z$ :

$$\mathcal{Y}_Z \frac{d\mathcal{D}}{dZ} = f_{\text{in}}(\mathcal{R}Z + \mathcal{Y}_Z) - (\beta_{\text{SN}} + \mathcal{R})\mathcal{D} + \frac{1}{\psi} \left[ \frac{dM_{\text{dust}}}{dt} \right]_{\text{acc}}. \quad (47)$$

In Method I,  $[dM_{\text{dust}}/dt]_{\text{acc}}/\psi = \mathcal{D}\xi(\tau_{\text{SF}}/\tau_{\text{grow}})$  (equation 30), where  $\tau_{\text{SF}} \equiv X_{\text{cl}}M_{\text{gas}}/\psi$  is the star formation time-scale. In Method II,  $[dM_{\text{dust}}/dt]_{\text{acc}}/\psi = \beta\mathcal{D}/\epsilon$  (equation 38). A large  $\tau_{\text{SF}}$  in Method I is equivalent with a small  $\epsilon$  in Methods II; that is, a small star formation efficiency means a long star formation time-scale. Because of this simple equivalence, we hereafter concentrate on Method II. Adopting Method II (i.e. equation 38), equation (47) is reduced to

$$\mathcal{Y}_Z \frac{d\mathcal{D}}{dZ} = f_{\text{in}}(\mathcal{R}Z + \mathcal{Y}_Z) - (\beta_{\text{SN}} + \mathcal{R} - \beta/\epsilon)\mathcal{D}. \quad (48)$$

Lada, Lombardi, & Alves (2010) show that the star formation efficiency in molecular clouds is roughly 0.1. They also mention that molecular clouds survive after the star formation activity over the last 2 Myr. The comparison with the age of stellar clusters associated with molecular clouds indicates that the lifetime of clouds is  $\sim 10$  Myr (Leisawitz, Bash, & Thaddeus 1989; Fukui & Kawamura 2010). Thus, we hereafter assume  $\epsilon = 0.1$  and  $\tau_{\text{mol}} = 10$  Myr as standard values. For the initial condition, we assume  $\mathcal{D} = 0$  and  $Z = 0$ .

The relations between dust-to-gas ratio and metallicity are shown in Fig. 8 for  $f_{\text{in}} = 0.1$  and in Fig. 9 for  $f_{\text{in}} = 0.01$ . We assume  $Z_{\odot} = 0.015$  (Lodders 2003). At low metallicity levels, the solution of equation (48) is approximated by  $\mathcal{D} \sim f_{\text{in}}Z$ . This is why the dust-to-gas ratio in the low-metallicity regime is lower in Fig. 9 than in Fig. 8. Above a certain metallicity level, a rapid increase of dust-to-gas ratio occurs because of the grain growth in clouds. The metallicity level at which this growth occurs is very sensitive to the grain size distribution.

The observational data of nearby galaxies are also shown for comparison. For the uniformity of data, we select the samples observed by *AKARI*: blue compact dwarf galaxies in Hirashita & Ichikawa (2009) and spiral galaxies (M 81 from Sun & Hirashita 2011 and M 101 from Suzuki et al. 2007). The dust masses are estimated from 90  $\mu\text{m}$  and 140  $\mu\text{m}$  data by using the mass absorption coefficient in Hirashita & Ichikawa (2009). For the gas mass of the dwarf galaxies and M 81, we adopt the H I mass, since the molecular mass is negligible or not detected. The H I masses of M 81 and of the dwarf galaxies are taken from Walter et al. (2008) and in Hirashita & Ichikawa (2009), respectively. For M 101, we adopt the sum of neutral and molecular gas masses compiled in Suzuki et al. (2007). The oxygen abundance is adopted for the indicator of the metallicity, and the solar abundance is assumed to be  $12 + \log(\text{O}/\text{H}) = 8.69$  (Lodders 2003). The oxygen abundances of the dwarf galaxies are compiled in Hirashita & Ichikawa (2009), and those of the spiral galaxies at the half-light radius are taken from Garnett (2002). Typical errors of the observational quantities are comparable to the size of symbols in the figures. To ensure that the *AKARI* results are not systematically different from other results, we add the data in Issa, MacLaren, & Wolfendale (1990), who estimated the dust mass from the extinction. The overall trend of the data is reproduced by the models.

Asano et al. (2011) also include a sample whose dust mass is derived from *Spitzer* observations by Engelbracht et al. (2008)

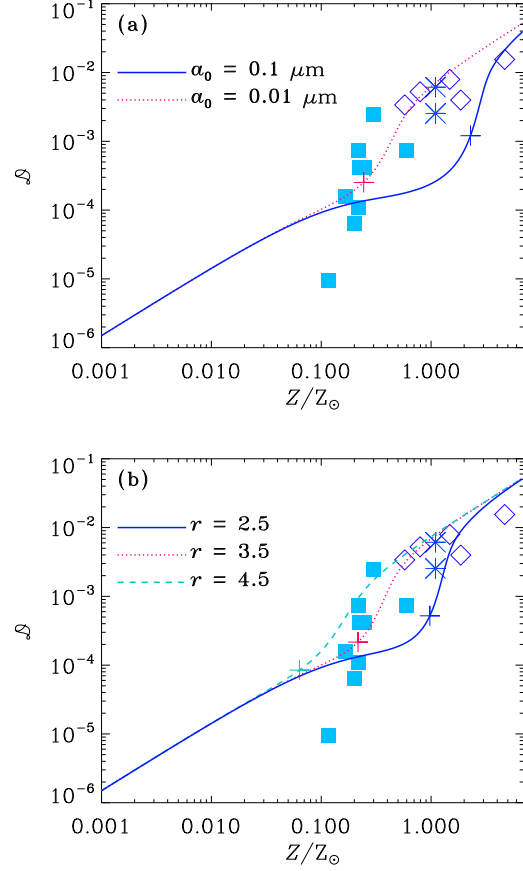


**Figure 8.** Relation between dust-to-gas ratio  $\mathcal{D}$  and metallicity  $Z$  for various grain size distributions with  $f_{\text{in}} = 0.1$ . (a)  $\delta$  function grain size distributions (the solid and dotted lines present the results for  $\alpha_0 = 0.1$  and  $0.01 \mu\text{m}$ , respectively). (b) Power-law grain size distributions (the solid, dotted, and dashed lines show the results for  $r = 2.5$ ,  $3.5$ , and  $4.5$ , respectively). The filled squares and asterisks represent the observational data for dwarf and spiral galaxies observed by *AKARI*, respectively (Hirashita & Ichikawa 2009; Suzuki et al. 2007; Sun & Hirashita 2011). The open diamonds are taken from Issa et al. (1990) as a spiral galaxy sample. The cross on each line marks the critical metallicity.

and show that the relation between dust-to-gas ratio and metallicity does not significantly change. The inclusion of *Herschel* data may boost the dust abundance because of the possible contribution from very cold dust especially in dwarf galaxies (Grossi et al. 2010). Galliano et al. (2005) also find a large contribution from very cold dust in the submillimetre for some dwarf galaxies. However, since the modeling of submillimetre emission may be significantly affected by the assumed emissivity index of large grains, we do not use the submillimetre data in this paper. We should keep in mind that that inclusion of submillimetre data can rather *decrease* the dust mass especially for dust-rich galaxies because the dust temperature estimate becomes better (Galametz et al. 2011). In their models, the *Spitzer* 160  $\mu\text{m}$  data are used; thus, it is not still unclear if there is a discrepancy between the dust temperatures estimated by *AKARI* and those estimated by including submillimetre data. The dust mass in M 81 derived by the *Herschel* observation ( $3.4 \times 10^7 M_{\odot}$ ; Bendo et al. 2010) is similar to that estimated by the *AKARI* observation adopted in this paper ( $3.2 \times 10^7 M_{\odot}$ ; Sun & Hirashita 2011).

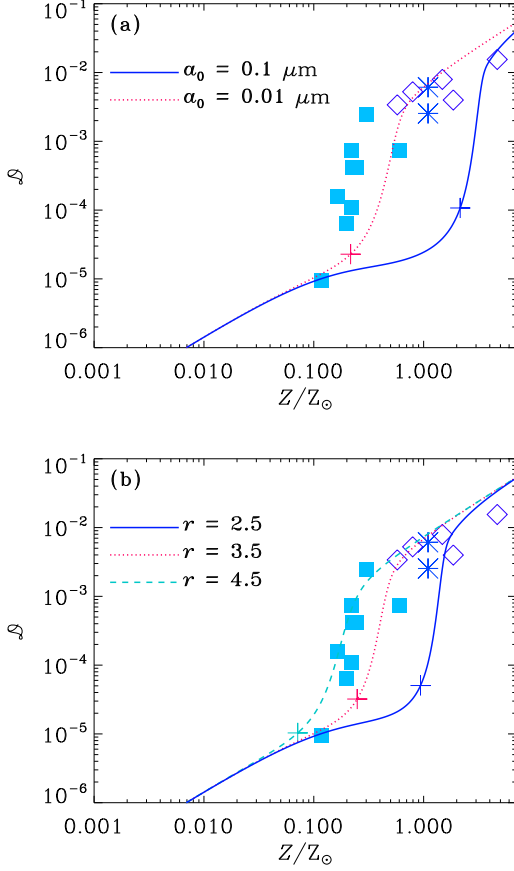


Figure 9. Same as Fig. 8 but for  $f_{\text{in}} = 0.01$ .

## 5 DISCUSSION

### 5.1 Effects of grain size distribution

We have shown that the grain size distribution significantly affects the evolution of dust mass above a certain metallicity level where the grain growth in clouds is activated. In fact, as shown in Figs. 8 and 9, the difference in the grain size distribution makes a significant imprint in the relation between dust-to-gas ratio and metallicity. This comes from the dependence of  $\beta$  on metallicity. As shown in equation (31),  $\beta \propto (\tau_{\text{grow}}/\tau_{\text{cl}})^{-1}$ . Fig. 6 shows that  $\tau_{\text{grow}}/\tau_{\text{cl}}$  is a decreasing function of metallicity. Thus,  $\beta$  increases as the system is enriched with metals, and if the last term in equation (48) becomes positive at a certain metallicity, the dust mass grows in a nonlinear way. Because  $\beta$  (or  $\tau_{\text{grow}}/\tau_{\text{cl}}$ ) is sensitive to the grain size distribution, the resulting relation between dust-to-gas ratio and metallicity depends largely on the grain size distribution. In other words, the metallicity level at which the grain growth in clouds is activated varies sensitively with the grain size distribution. This metallicity level is called ‘critical metallicity’, which is quantified and discussed in the next subsection.

### 5.2 Critical metallicity for the grain growth

Asano et al. (2011) and Inoue (2011) have shown that the grain growth by accretion dominates the grain abundance if the metallicity is larger than a certain ‘critical metallicity’. As mentioned in the previous subsection, the nonlinear increase of dust-to-gas ratio

Table 3. Critical metallicities for grain growth.

$n^a$	$a_0$ [ $\mu\text{m}$ ]	$r$	$a_{\text{min}}$ [ $\mu\text{m}$ ]	$a_{\text{max}}$ [ $\mu\text{m}$ ]	$Z_{\text{cr}}$ [ $Z_{\odot}$ ]
$\delta$	0.1	—	—	—	2.3
$\delta$	0.01	—	—	—	0.24
p	0.1	3.5	0.001	0.25	0.22
p	0.1	2.5	0.001	0.25	0.97
p	0.1	4.5	0.001	0.25	0.063
p	0.1	3.5	0.0003	0.25	0.094
p	0.1	3.5	0.003	0.25	0.45

<sup>a</sup> Grain size distribution: “p” for the power law and “ $\delta$ ” for the  $\delta$  function.

by grain growth is realized when  $-\beta_{\text{SN}} - \mathcal{R} + \beta/\epsilon > 0$  in equation (48). Since  $\beta_{\text{SN}} \gg \mathcal{R}$ , the critical metallicity,  $Z_{\text{cr}}$ , can be estimated by the metallicity at which  $\beta$  as a function of metallicity realizes

$$\beta(Z_{\text{cr}}) = \epsilon\beta_{\text{SN}}, \quad (49)$$

where  $\beta(Z)$  indicates that  $\beta$  is a function of metallicity. In our models,  $\epsilon = 0.1$  and  $\beta_{\text{SN}} = 9.65$ , i.e.,  $\beta(Z_{\text{cr}}) = 0.965$ . Therefore, if the metallicity is so high that the grain growth in individual clouds increases the dust mass by 0.965 times the original dust amount, the grain growth becomes prominent. The critical metallicity varies by a factor of  $\sim 1.5$  if we change  $\beta_{\text{SN}}$  by a factor of 2 (i.e. uncertainty in  $\beta_{\text{SN}}$  from the assumed species; Jones & Nuth 2011).

The position for the critical metallicity is marked on each line in Figs. 8 and 9 and listed in Table 3 (for  $f_{\text{in}} = 0.1$  but  $Z_{\text{cr}}$  only decrease by  $\sim 10$ –20 per cent for  $f_{\text{in}} = 0.01$ ). Indeed the dust-to-gas ratio rapidly increases if the metallicity becomes larger than the critical metallicity. This supports Inoue (2011)’s view that the activation of grain growth is driven by the metallicity. In this paper we have found that the critical metallicity is sensitive to the grain size distribution. If the major part of the grains are as large as  $\sim 0.1 \mu\text{m}$ , the grain growth is activated above  $\sim 2 Z_{\odot}$ , which is too large to explain the large grain abundance in the objects with sub-solar metallicities. If the typical grain size is as small as  $\sim 0.01 \mu\text{m}$  or the grain size distribution is described by a power law with  $r \gtrsim 3.5$ , the large grain abundance in sub-solar metallicity galaxies can be naturally explained by the efficient grain growth in clouds. Therefore, the evolutionary history of grain size distribution is important to understand the grain abundance in galaxies.

By an analysis of infrared dust emission spectra, Galliano et al. (2005) show that the grain size distributions of some metal-poor dwarf galaxies are biased toward smaller grains compared with the Galactic case (i.e.  $r \simeq 3.5$ ). Therefore, the critical metallicity for these dwarf galaxies is expected to be lower than their metallicities: in other words, the grain growth in clouds is expected to contribute significantly to the dust abundance in these galaxies. It is interesting to point out that  $r = 4.5$  explains the data points of metal-poor galaxies better than  $r = 3.5$ . This is consistent with Galliano et al. (2005)’s conclusion that the grain size distribution is biased to small sizes.

After the grain growth, all the lines in Figs. 8 and 9 finally converge. This is explained as follows. If the metallicity is high enough, the grain growth is regulated by the lifetime of clouds and is independent of grain size distribution. In other words,  $\beta \sim \xi/(1 - \xi)$  if the metallicity becomes high enough (i.e.  $y$  is large enough in equation 36). Using  $\xi = 1 - \mathcal{D}/Z$  and equation (48), we obtain the following estimate in the case where the grain growth

dominates the increase of the dust content:

$$\begin{aligned} \mathcal{V}_Z \frac{d\xi}{dZ} &\sim (\beta_{\text{SN}} - \beta/\epsilon) \frac{\mathcal{D}}{Z^2} \\ &\sim \left( \beta_{\text{SN}} - \frac{1}{\epsilon} \frac{\xi}{1-\xi} \right) \frac{\mathcal{D}}{Z^2}, \end{aligned} \quad (50)$$

which is valid for  $Z > Z_c$  (we only adopt the dominant terms). Therefore, if  $\xi$  is so small (large) that the right-hand side of this equation is positive (negative),  $\xi$  tends to increase (decrease) as  $Z$  increases. This means that  $\xi$  tends to approach the value that makes the right-hand side to be zero; that is,

$$\xi \sim \frac{\epsilon\beta_{\text{SN}}}{1 + \epsilon\beta_{\text{SN}}} \quad \text{for } Z \gg Z_{\text{cr}}. \quad (51)$$

For the values adopted in our models ( $\epsilon = 0.1$  and  $\beta_{\text{SN}} = 9.65$ ),  $\xi \sim 0.49$ . This means that the fraction of metals in dust phase is about 0.5 at metallicities much higher than the critical metallicity. If we consider the uncertainty in  $\beta_{\text{SN}}$  by a factor of 2 because of material difference (Jones & Nuth 2011),  $\xi \sim 0.33\text{--}0.66$ .

It is interesting that  $\xi$  at  $Z \gg Z_{\text{cr}}$  only depends on  $\epsilon\beta_{\text{SN}}$ . Using the definition of  $\beta_{\text{SN}} = \epsilon_s M_s \gamma / \psi$  (below equation 44) and equation (37), we obtain

$$\epsilon\beta_{\text{SN}} = \frac{\epsilon_s M_s \gamma}{X_{\text{cl}} M_{\text{gas}} / \tau_{\text{cl}}}. \quad (52)$$

This is the ratio between the gas mass swept by SN shocks per unit time multiplied by the efficiency of dust destruction in SN shocks, and the formation rate of clouds. In other words, this is the ratio between the dust destruction rate by SN shocks and the grain growth rate in clouds. Therefore, it is natural that the final fraction of metals in dust phase can be described by the balance between the dust destruction by SN shocks and the dust formation in clouds.

Inoue (2011) also obtained a similar expression for the critical metallicity. We have confirmed his conclusion that the dust-to-metal ratio approaches a constant value: this behaviour is called self-regulation by Inoue (2011). The difference between our formulation and his is that he treated  $\tau_{\text{SF}}$  as a parameter independent of  $\tau_{\text{grow}}$  while we connect these two parameters through the star formation efficiency  $\epsilon$ . Since both star formation and grain growth occur in molecular clouds, these two processes are not independent. Moreover, if the grain growth is efficient enough, the dust growth time-scale is limited by the lifetime of clouds, which is independent of the grain size distribution. Therefore, the dust-to-metal ratio does not depend on the grain size distribution for  $Z \gg Z_{\text{cr}}$ , and it depends only on  $\epsilon\beta_{\text{SN}}$ .

### 5.3 Significance in galaxy evolution

The first dust should be produced by SNe in the death of massive stars. Because of shock destruction in SNe, the dust sizes may be biased to  $a \gtrsim 0.1 \mu\text{m}$  (Bianchi & Schneider 2007; Nozawa et al. 2007). Hirashita et al. (2010) show that shattering driven by interstellar turbulence can produce small grains efficiently if the metallicity becomes higher than a critical value ( $\sim 0.1\text{--}1 Z_{\odot}$ ). Thus, the critical metallicity for the grain growth is near the metallicity level where shattering produces small grains efficiently. The production of small grains accelerates the grain growth by accretion, which raises the grain abundance. With the increased dust abundance, shattering can be further efficient, although the produced small grains by shattering does not necessarily activate further shattering of large grains (Jones et al. 1996). Such an interplay between

shattering and accretion may be interesting to investigate in the future.

The size distribution of grains produced by AGB stars is also important since AGB stars become the dominant dust production source after several hundreds of Myr (Valiante et al. 2009; Gall et al. 2011a; Asano et al. 2011). The size of grains produced in AGB stars is suggested to be large ( $a \sim 0.1 \mu\text{m}$ ) from the observations of spectral energy distributions (Groenewegen 1997; Gauger et al. 1999), although Hofmann et al. (2001) show that the grains are not single-sized. To clarify the grain size distribution formed by AGB stars is important for the efficiency of grain growth. Shattering in the ISM may also play a role in efficiently producing small grains even if AGB stars only produce large grains (Hirashita 2010). In this case, efficient grain growth can occur.

It is interesting to point out that the critical metallicity is within the metallicity range typical of dwarf galaxies (Table 3). This confirms the conclusion by Asano et al. (2011) that the strong metallicity dependence of the dust-to-gas ratio in dwarf galaxies can be explained by the grain growth in clouds.

The grain growth is also important in some high-redshift galaxy populations. In fact, high-redshift quasars have solar (or more) metallicities (e.g. Juarez et al. 2009), which implies that the grain growth is indeed governing the dust abundance in distant quasars (Michalowski et al. 2010; Pipino et al. 2011; Asano et al. 2011) (but see Valiante et al. 2009; Gall et al. 2011b). If the abundance of small grains are enhanced because of shattering as suggested by Hirashita et al. (2010), the critical metallicity becomes lower, so that the importance of grain growth in clouds is further pronounced.

Qualitatively it may be predicted that the mid-infrared emission from very small grains is relatively suppressed if the grain growth in clouds is activated. However, it is hard to quantitatively predict the galaxy-scale observational features caused by the grain growth in clouds because it is difficult to selectively see the clouds, where grain growth is occurring. Since observations of galactic spectral energy distribution inevitably include the emission from diffuse medium, other mechanisms modifying the grain size distribution such as shattering and coagulation are also reflected in the observed emission from grains. Indeed, Galliano et al. (2005) show that the grain size distribution is biased toward smaller grains in some dwarf galaxies, which may be interpreted as the efficient grain processing in diffuse medium. They also demonstrate that there is a variety in the grain size distribution among dwarf galaxies. Such a variety will be investigated in the future with a consistent treatment of a nonlinear combination between the small grain production by shattering and sputtering and the grain growth by accretion and coagulation.

## 6 CONCLUSION

We have formulated and investigated the grain growth rate by accretion in interstellar clouds. The formalism is applicable to any grain size distribution. We have found that the grain size distribution is really fundamental in regulating the grain growth rate. We have also implemented the formulation of grain growth in individual clouds into the chemical evolution models of entire galaxies. The models also treat dust supply from stellar sources and dust destruction by SN shocks, but we have focused particularly on the grain growth in clouds in this paper. We have found that the metallicity level where the grain growth in clouds becomes dominant strongly depends on the grain size distribution. If the significant

fraction of the grains have radii  $\lesssim 0.01 \mu\text{m}$  or the grain size distribution is described as power law with  $r \gtrsim 3.5$ , the large grain abundance at the sub-solar metallicity level is naturally explained by the grain growth in clouds because the surface-to-volume ratio of the grains is large enough. The grain growth should be efficient in galaxies whose metallicity is above  $Z_{\text{cr}}$  estimated in Section 5.2. Our formulation for the grain growth is applicable to any grain size distribution and is implemented straightforwardly into any framework of chemical enrichment models.

## ACKNOWLEDGMENTS

We are grateful to the referee, A. P. Jones, for useful comments, which improved the discussion in this paper very much. We thank A. K. Inoue for helpful discussions on dust evolution in galaxies. H.H. is supported by NSC grant 99-2112-M-001-006-MY3.

## REFERENCES

- Asano, R. S., Takeuchi, T. T., Hirashita, H., & Inoue, A. K. 2011, *A&A*, submitted
- Bendo, G. J., et al. 2010, *A&A*, 518, L65
- Bianchi, S., & Schneider, R. 2007, *MNRAS*, 378, 973
- Calura, F., Pipino, A., & Matteucci, F. 2008, *A&A*, 479, 669
- Compiègne, M. et al. 2011, *A&A*, 525, A103
- Désert, F.-X., Boulanger, F., & Puget, J. L. 1990, *A&A*, 237, 215
- Draine, B. T. 2009, in Henning Th., Grün E., Steinacker J., eds, *Cosmic Dust – Near and Far*. ASP Conf. Ser., ASP, San Francisco, p. 453
- Draine, B. T., & Lee, H. M. 1984, *ApJ*, 285, 89
- Dwek, E. 1998, *ApJ*, 501, 643
- Engelbracht, C. W., Rieke, G. H., Gordon, K. D., Smith, J.-D. T., Werner, M. W., Moustakas, J., Willmer, C. N. A., & Vanz, L. 2008, *ApJ*, 678, 804
- Evans, A. 1994, *The Dusty Universe*, Wiley, Chichester
- Fukui, Y., & Kawamura, A. 2010, *ARA&A*, 48, 547
- Galametz, M., Madden, S. C., Galliano, F., Bendo, G. J., & Sauvage, M. 2011, *A&A*, in press
- Gall, C., Andersen, A. C., & Hjorth, J. 2011a, *A&A*, 528, A13
- Gall, C., Andersen, A. C., & Hjorth, J. 2011b, *A&A*, 528, A14
- Galliano, F., Madden, S. C., Jones, A. P., Wilson, C. D., & Bernard, J.-P. 2005, *A&A*, 434, 867
- Galliano, F., Madden, S. C., Jones, A. P., Wilson, C. D., Bernard, J.-P., & Le Peintre, F. 2003, *A&A*, 407, 159
- Garnett, D. R. 2002, *ApJ*, 581, 1019
- Gauger, A., Balega, Y. Y., Irrgang, P., Osterbart, R., & Weigelt, G. 1999, *A&A*, 346, 505
- Govazzi, G., Bonfanti, C., Sanvito, G., Boselli, A., & Scodreggio, M. 2002, *ApJ*, 576, 135
- Grassi, T., Krstic, P., Merlin, E., Buonomo, U., Piovan, L., & Chiosi, C. 2011, *A&A*, in press
- Groenewegen, M. A. T. 1997, *A&A*, 317, 503
- Grossi, M., et al. 2010, *A&A*, 518, L52
- Guillet, V., Pineau des Forêts, G., & Jones, A. P. 2007, *A&A*, 476, 263
- Guillet, V., Pineau des Forêts, G., & Jones, A. P. 2011, *A&A*, 527, A123
- Hirashita, H. 2000a, *PASJ*, 52, 585
- Hirashita, H. 2000b, *ApJ*, 531, 693
- Hirashita, H. 2010, *MNRAS*, 407, L49
- Hirashita, H., & Ichikawa, T. T. 2009, *MNRAS*, 396, 500
- Hirashita, H., Nozawa, T., Yan, H., & Kozasa, T. 2010, *MNRAS*, 404, 1437
- Hirashita, H., & Yan, H. 2009, *MNRAS*, 394, 1061
- Hofmann, K.-H., Balega, Y., Blöcker, T., & Weigelt, G. 2001, *A&A*, 379, 529
- Inoue, A. K. 2003, *PASJ*, 55, 901
- Inoue, A. K. 2011, *Earth, Planets, and Space*, submitted
- Issa, M. R., MacLaren, I., & Wolfendale, A. W. 1990, *A&A*, 236, 237
- Jones, A. P., & Nuth, J. A., III 2011, *A&A*, submitted
- Jones, A. P., Tielens, A. G. G. M., & Hollenbach, D. J. 1996, *ApJ*, 469, 740
- Jones, A., Tielens, A. G. G. M., Hollenbach, D. J., McKee, C. F. 1994, *ApJ*, 433, 797
- Juarez, Y., Maiolino, R., Mujica, R., Pedani, M., Marinoni, S., Nagao, T., Marconi, A., & Oliva, E. 2009, *A&A*, 494, L25
- Kennicutt, R. C., Jr. 1998, *ARA&A*, 36, 189
- Kozasa, T., Nozawa, T., Tominaga, N., Umeda, H., Maeda, K., & Nomoto, K. 2009, in Henning Th., Grün E., Steinacker J., eds, *Cosmic Dust – Near and Far*. ASP Conf. Ser., ASP, San Francisco, p. 43
- Lada, C. J., Lombardi, M., & Alves, J. F. 2010, *ApJ*, 724, 687
- Leisawitz, D., Bash, F. N., & Thaddeus, P. 1989, *ApJS*, 70, 731
- Leitch-Devlin, M. A., & Williams, D. A. 1985, *MNRAS*, 213, 295
- Lisenfeld, U., & Ferrara, A. 1998, *ApJ*, 496, 145
- Lodders, K. 2003, *ApJ*, 591, 1220
- Mathis, J. S., Rumpl, W., & Nordsieck, K. H. 1977, *ApJ*, 217, 425 (MRN)
- McKee, C. F. 1989, in Allamandola L. J. & Tielens A. G. G. M. eds., *IAU Sump. 135, Interstellar Dust*, Kluwer, Dordrecht, 431
- Michałowski, M. J., Murphy, E. J., Hjorth, J., Watson, D., Gall, C., & Dunlop, J. S. 2010, *A&A*, 522, A15
- Nozawa, T., Kozasa, T., Habe, A., Dwek, E., Umeda, H., Tominaga, N., Maeda, K., & Nomoto, K. 2007, *ApJ*, 666, 955
- O'Donnell, J. E., & Mathis, J. S. 1997, *ApJ*, 479, 806
- Ormel, C. W., Paszun, D., Dominik, C., & Tielens, A. G. G. M. 2009, *A&A*, 502, 845
- Pipino, A., Fan, X. L., Matteucci, F., Calura, F., Silva, L., Granato, G., & Maiolino, R. 2011, *A&A*, 525, A61
- Savage, B. D., & Sembach, K. R. 1996, *ARA&A*, 34, 279
- Serra Díaz-Cano, L., & Jones, A. P. 2008, *A&A*, 492, 127
- Sun, A.-L., & Hirashita, H. 2011, *MNRAS*, 411, 1070
- Suzuki, T., Kaneda, H., Nakagawa, T., Makiuti, S., & Okada, Y. 2007, *PASJ*, 59, 473
- Valiante, R., Schneider, R., Bianchi, S., & Andersen, A. C. 2009, *MNRAS*, 397, 1661
- Walter, F., Brinks, E., de Blok, W. J. G., Bigiel, F., Kennicutt, R. C., Thornley, M. D., & Leroy, A. 2008, *AJ*, 136, 2563
- Weingartner, J. C., & Draine, B. T. 1999, *ApJ*, 517, 292
- Weingartner, J. C., & Draine, B. T. 2001, *ApJ*, 548, 296
- Yamasawa, D., Habe, A., Kozasa, T., Nozawa, T., & Hirashita, H. 2011, *ApJ*, in press
- Yan, H., Lazarian, A., & Draine, B. T. 2004, *ApJ*, 616, 895
- Zhukovska, S., Gail, H.-P., & Tieloff, M. 2008, *A&A*, 479, 453

## APPENDIX A: INSTANTANEOUS RECYCLING APPROXIMATION

We estimate  $\mathcal{R}$  and  $\mathcal{Y}_Z$  used in Section 4.4. With an initial mass function (IMF)  $\phi(m)$ ,  $\mathcal{R}$  and  $\mathcal{Y}_Z$  are written as

$$\mathcal{R} = \int_{m_t}^{m_u} [m - w(m)] \phi(m) dm, \quad (\text{A1})$$

$$\mathcal{Y}_Z = \int_{m_t}^{m_u} m p_Z(m) \phi(m) dm, \quad (\text{A2})$$

where  $m_t$  is the turn-off stellar mass,  $m_u$  is the upper mass cutoff of stellar mass,  $m$  is the stellar mass,  $w_m$  is the remnant mass,  $p_Z(m)$  is the fraction of mass converted into metals in a star of mass  $m$ . We assume the Salpeter IMF ( $\phi(m) \propto m^{-2.35}$ ) with stellar mass range  $0.1 M_\odot \leq m \leq 100 M_\odot$ . The IMF is normalized as

$$\int_{m_l}^{m_u} m \phi(m) dm = 1, \quad (\text{A3})$$

where  $m_l$  is the lower mass cutoff of stellar mass.

For the remnant mass, we adopt the fitting formula provided by Inoue (2011):

$$\frac{w(m)}{m} = \begin{cases} 1 & (m > 40 M_\odot), \\ 0.13 \left( \frac{m}{8 M_\odot} \right)^{-0.5} & (8 \leq m \leq 40 M_\odot), \\ 0.13 \left( \frac{m}{8 M_\odot} \right)^{-0.7} & (m < 8 M_\odot). \end{cases} \quad (\text{A4})$$

We also adopt the fitting formula for the mass of ejected metals as a function of stellar mass as (Inoue 2011)

$$\frac{m_Z(m)}{m} = \begin{cases} 0 & (m > 40 M_\odot), \\ 0.02 \left( \frac{m}{8 M_\odot} \right)^2 & (8 \leq m \leq 40 M_\odot), \\ 0.02 \left( \frac{m}{8 M_\odot} \right)^{0.7} & (m < 8 M_\odot). \end{cases} \quad (\text{A5})$$

Inoue (2011) show that there is no trend with metallicity  $Z$  for  $m_Z/m$ . In fact,  $m_Z$  is the mass of ejected metals, so we need to subtract the metal mass already included before the nucleosynthesis:  $m p_Z(m) = m_Z(m) - Z[m - w(m)]$ . Since the metallicity range of interest is  $0 \leq Z \lesssim 0.02$ ,  $m p_Z(m)$  is reasonably between  $m_Z(m) - 0.02[m - w(m)]$  (called minimum) and  $m_Z(m)$  (maximum). In Fig. A1, we show  $\mathcal{R}$  and  $\mathcal{Y}_Z$  as a function of the turn-off mass (or age). We adopt the values at  $t = 5$  Gyr, that is,  $\mathcal{R} = 0.18$  and  $\mathcal{Y}_Z = 0.013$  (average of the maximum and the minimum), since the typical gas consumption time-scale or star formation time-scale of nearby star-forming galaxies is 1–10 Gyr (Kennicutt 1998; Gavazzi et al. 2002). However, the uncertainty caused by the age is within a factor of 2 if we adopt an age of  $> 4 \times 10^7$  yr. Thus, as long as we treat galaxies whose typical star formation time-scale is longer than a few  $\times 10^7$  yr, our calculation gives a reasonable results for the metal and dust enrichment.

The SN rate,  $\gamma$ , is also necessary to estimate the dust destruction rate. If we assume that stars with  $m \geq 8 M_\odot$  become SNe,  $\gamma$  can be related to the star formation rate by approximating the lifetimes of these stars to be zero:

$$\gamma = \psi \int_{8 M_\odot}^{m_u} \phi(m) dm = 0.00742 (M_\odot^{-1}) \psi. \quad (\text{A6})$$

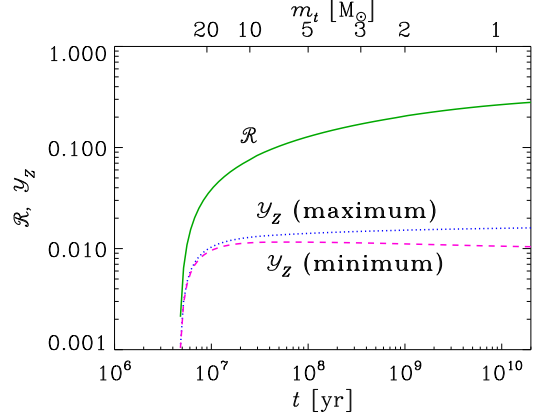


**Figure A1.** The returned fraction of gas  $\mathcal{R}$  (solid line) and the fraction of newly produced metals  $\mathcal{Y}_Z$  (dotted and dashed lines) are shown as a function of turn-off stellar mass or age. For  $\mathcal{Y}_Z$ , the maximum (dotted line) and the minimum (dashed line) cases are shown.

This paper has been typeset from a  $\text{\LaTeX}$  file prepared by the author.